Supporting Information for

Centrochirality induces exceptionally high CISS by the sergeant and soldier effect: achiral poly(amino acid)s as transducers of chiral information.

Content

1. Materials

The chiral amines *R*- and *S*-1,2,3,4-tetrahydronaphthalen-1-amine and alpha-pinene were purchased from Sigma-Aldrich and were used without further purification. Triphosgene and 2-aminoisobutyric acid were purchased from ABCR. The corresponding amino acid *N*-carboxyanhydride (NCA) was synthesized by a triphosgene reaction as described in the literature.

All solvents were dried prior to use. DMF and THF were passed through a solvent purifying system. Hexane was dried over sodium and benzophenone and was freshly distilled under nitrogen atmosphere prior to use. Ethyl acetate was dried over P_2O_5 and distilled under nitrogen atmosphere prior to use.

2. Methods

Matrix-assisted laser desorption/ionization time-of-flight mass spectrometry (MALDI-ToF MS) measurements were performed on a Bruker Autoflex III system (Bruker Daltonics) using a nitrogen laser operating at a wavelength of λ = 337 nm in reflection mode. The used matrix:analyte:salt ratio was 100:10:1 and 1 µL of the solution was spotted on the MALDI target. The polymer samples were either dissolved or suspended in HFIP or DMF with a concentration of 20 mg/mL and dithranol was used as matrix adjusting a concentration of 20 mg/mL in THF, while NaTFA was used as salt with a concentration of 20 mg/mL in THF. Data evaluation was carried out via flexAnalysis software (3.4) and simulation of the isotopic pattern was performed by Data Analysis software (version 4.0).

CD Spectroscopy was performed on a JASCO J-1500 with a PTC-510 cell holder. For measurements a 1 mm cuvette with a sample concentration of c = 0.2 mg/mL was used at a wavelength range from 185 nm to 260 nm with a scanning speed of 100 nm/min with 20 accumulations. Baseline subtraction of the corresponding solvent has been conducted to obtain the corrected spectra. The measurements were conducted in HFIP. Data analysis was performed by Spectra Analysis program from JASCO.

Gel permeation chromatography (GPC) was conducted by a system in 1,1,1,3,3,3-Hexafluroisopropan-2-ol.
HFIP-based SEC measurements with 0,1 mol/l KTFAc were performed at 35 °C on a Viscotek GPCmax VE 2001 from Malvern applying a PSS PFG precolumn and a PSS PFG main column. As solvent HFIP with 0,1 mol/l KTFAc was used and the sample concentration was adjusted to appr. 3 mg mL^{-1} while applying a flow rate of 1 mL min^{-1}. The refractive index detection was performed with a VE 3580 RI detector of ViscotekTM. For determination of the molecular weights, external calibration was done using polymethyl methacrylate (PMMA) standards (purchased form PSS) with a molecular weight range from 602 to 62.200 g mol^{-1}. OmniSEC software (Version 5.12.) was used for evaluating data.

Attenuated reflection Infrared spectroscopy (ATR-IR)
Fourier-transform infrared spectroscopy measurements were done on a Bruker Tensor VERTEX 70 spectrometer and Opus 8.2 was used for data analysing. For Attenuated total reflection-infrared (ATR-FTIR), a Golden Gate Heated Diamond ATR Top-plate was equipped and the sample was applied as a solid powder. Before the measurement a background spectra was measured and subtracted of the spectra measured afterwards.

Nuclear magnetic spectroscopy (NMR) was conducted on a Varian Gemini 400 NMR spectrometer (400 or 500 MHz) at 27 °C while using deuterated HFIP solvent as lock and the residual solvent signal as internal reference. All chemical shifts are given in ppm and all coupling constants in Hz. For interpretation of NMR-data MestReNova software (Version 11.0.0.17609) was used.

X-ray photoelectron spectroscopy (XPS) was conducted on a K-Alpha^{+} Surface Analysis from Thermo Fischer Scientific using the Thermo Avantage software version 5.9925. The measured spot size was 400 µm with an energy step size of 0.1 eV and a pass energy of 50 eV. The dwell time for the measurement was 50 seconds and each measurement consists of 10 scans. The obtained data was then displayed in Origin software.

Atomic force microscopy (AFM) was performed using a nanosurf CoreAFM with Tap190AI-G Cantilevers in the Phase-contrast mode. The vibrational amplitude was set to 1 V. As parameter while measuring a P-Gain of 1500, I-Gain of 1000 and D-Gain of 0 was used with a time per line of 1 s. Data analysis was done using Gwyddion 2.53 (freeware, http://gwyddion.net/).

Vibrating sample magnetometer (VSM) measurements were conducted on a '8600 Series VSM system' from 'Lake Shore Cryotronics, Inc' to investigate the perpendicular magnetic anisotropy (PMA) of the thin layer heterostructure. The head position for the measurement was 8.5 mm above the surface and an averaging time of 500 ms was used.

Preparation of magnetic thin film heterostructure with PMA layer was done using the magnetron sputtering system.
For the preparation of the films, a home-built MANGO (multi-source, atomically engineered, next generation, alloys and compounds deposition system) physical vapor deposition system was used, which has a base pressure of < 10^{-9} Torr. Deposition was carried out at room temperature in an Argon atmosphere of 3 mTorr on n-doped Si substrate. The ferromagnet (FM) film stack is as follows: n-doped Si||20 TaN|20 Pt|3 Co|7 Ni|3 Co|20 Au (units in Å) with the Co/Ni/Co structure acting as the PMA layer.

Laser lithography (MLA 150, Heidelberg Instruments) was used to expose the makers with number coordinates on the gold surface of the PMA substrate with positive photoresist (ARP3540T).

Conducting atomic force microscopy (c-AFM) was propped on a cypher scanning probe microscope model blue drve/ES/enclosure system. As a tip a n+-silicon cantilever with a Pt/Ir-coated tip was used. The tip has a height of 10-15 µm and a resistivity of 0.01-0.02 Ω*cm. The cantilever has a length of 225 µm, a width of 48 µm, a thickness of 1 µm and a force constant of 0.01-1.87 N/m. To ensure

the quality of the tip remains the same, before and after the c-AFM measurements the conductivity of the tip was determined by measuring a pure gold surface (see supplementary Fig. SI 14). The voltage was applied between the magnetized substrate and the c-AFM tip starting from 0 V going up to 0.2 V and down to -0.2 V back to 0 V with a 0.2 Hz frequency for this sweep. All current measurements were conducted in contact mode after a successful tip approach. For a statistical analysis multiple voltage sweeps were conducted per measured spot on the substrate surface (see supplementary table SI 1).

The feedback mechanism of the AFM system causes the AFM tip to approach or retract from the sample surface when measuring the I-V curve. When the detected current is too high, the tip gradually moves away from the sample surface, while when the current is too low, the tip gradually approaches the sample surface. This results in significant difference in the I-V curve during multiple measurement which in the worst case can lead to a complete loss or sudden increase of the conductivity. Meanwhile, since the lengths of these synthesized polymers vary (with Aib chains ranging from 10 to 20 repeating units), the current distribution through these polymers will differ each time, even when the same bias voltage is applied to the same region. For example, when a larger proportion of the current flows through shorter polymers, the measured current will be higher, whereas when a larger proportion flows through longer polymers, the measured current will be lower. This explains the high deviation of measurement results shown in Fig 6. I-V curves which show either no conductivity at all, a loss or a sudden increase of conductivity during the measurement were sorted out and not used for further investigations.

Table SI 1: Number of I-V sweeps performed with c-AFM on the polymer coated gold surface of the PMA substrate. The raw data is shown in Fig. 6 a, b, d and e for the *R*- and *S*-Polymer with up and down Magnetization respectively.

	R-Polymer (*M*-3_{10}-helix))	*S*-Polymer (*P*-3_{10}-helix)
Down Magnetization	74 measurements	137 measurements
Up Magnetization	96 measurements	94 measurements

3. Synthetic procedures

Aib-NCA was synthesized according to a former published procedure.[1]

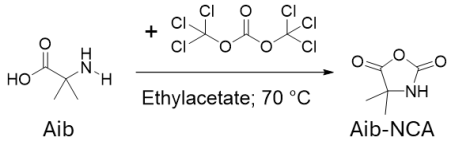

Scheme SI 1: Synthesis of Aib-NCA with triphosgene and Aib in ethylacetate at 70°C for 3 days.

2-Aminoisobutyric acid (Aib) (15 g, 145 mmol) and alpha-pinene (39.6 g, 290.7 mmol) were suspended in dried ethyl acetate (110 mL) and heated to 80°C. Triphosgene (29.3 g, 98.8 mmol) was dissolved in a small amount of ethyl acetate (20 mL) and added via a syringe to the flask. The reaction was stirred for 3 days under reflux condensation and nitrogen atmosphere until the solution was completely clear. The remaining phosgene was removed by purging the solution with nitrogen and removing most of the solvent. The Aib-NCA was precipitated by adding cold Hexane. The formed white needles were filtered and washed with hexane and consequently dried in vacuum yielding white needles as product (~ 60% yield).

Polymerization of Aib-NCA with chiral amines was conducted according to a previously published method.[1a]

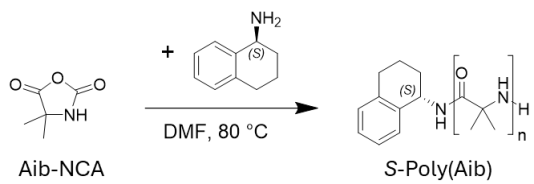

Scheme SI 2: Synthetic scheme for the polymerization of Aib-NCA using the *S*-1,2,3,4-tetrahydronaphthalen-1-amine as chiral amine initiator yielding the *S*-Poly(Aib) as a product.

Aib-NCA (200 mg, 1.55 mmol) was dissolved in dry DMF (0.6 mL) under nitrogen atmosphere. The chiral amine (15 µL, 0.1 mmol) was added via an Eppendorf pipette and stirred over night at 80°C. The polymer precipitated during the reaction forming a white suspension. The polymer was purified by dialysis in acetone with a molecular weight cut off of 1000 g/mol for 3 days. The polymer was dried in vacuum and obtained as a white powder (92 mg, ~ 70% yield).

End group modification of polymer

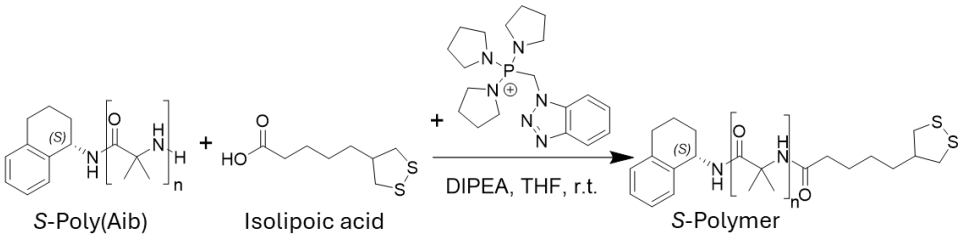

Scheme SI 3: Synthetic scheme of the post functionalization of the *S*-Poly(Aib) with isolipoic acid by a peptide coupling reaction with PyBOP as coupling agent and DIPEA as base in THF at room temperature for 3 days yielding the *S*-Polymer as a product.

Isoliopic acid (6.6 mg, 0.032 mmol) was dissolved in dry THF (1.5 mL) and PyBOP (20 mg, 0.038 mmol) and DIPEA (12.4 mg, 16.3 µL, 0.096 mmol) were added to activate the acid group. The *R*- or *S*-initiated Poly(Aib) (40 mg, 0.032 mmol) was added and suspended in the solution. After stirring for 3 days at room temperature the polymer was purified by dialysis in acetone with a molecular cut off of 1000 g/mol for 3 days. The product was dried in vacuum yielding a white powder (35 mg, ~ 75 % yield).

Formation of polymer self-assembled monolayer

The PMA substrate with gold surface was cleaned prior polymer application. The substrate was put in boiling acetone and ethanol for 10 minutes and afterwards dried with a nitrogen stream. The surface of the PMA substrate was cleaned in a UV ozone cleaner for 5 minutes and immediately submerged in a 2 mg/mL sulphur end capped polymer solution (*R*-/*S*-Polymer) in HFIP. After 1 day the substrate was removed from the solution and washed with pure HFIP to remove unbound polymer. The substrate with the polymer coating was dried and characterized with XPS and AFM.

Chiral induced spin selectivity measurements

The PMA substrate with polymer coating was investigated with AFM to prove a polymer layer in the investigated area. With a roughness above 1 nm the presence of the polymer was confirmed before measuring a current-voltage sweep in this area with c-AFM. The PMA layer was magnetized in one of two possible directions by holding a strong magnet with the N or S pole side in close proximity to the surface for at least 30 seconds. The surface was approached with the c-AFM tip as close as possible and the measurement was performed in contact mode. The current which was transferred between the thin layered heterostructure stack and the AFM tip was measured depending on the applied voltage. One polymer coated PMA substrate was measured multiple times on at least 5 different spots on the surface. The magnetization was switched to the other direction by holding the opposite side of the magnet close to the substrate surface. The c-AFM measurements were conducted again now with the opposite magnetization of the PMA layer with at least 5 spots in a similar area measured. The results were later averaged and compared between the magnetization directions to calculate the CISS effect of the investigated polymer.

4. Supporting data

4.1. CD data

CD spectroscopy was used to prove the successful chiral induction using the chiral amines as a head group. The CD spectra of the initiator differs significantly from the CD spectra of the *R*- and *S*-Poly(Aib) which show a mirroring behaviour along the CD = 0 line. The *R*- and *S*-Polymers show no significant difference to the unmodified *R*- and *S*-Poly(Aib) which shows that there is no effect of the achiral isolipoic acid on the secondary structure of the polymer. The *R*-initiator seems to induce a left-handed *M*-helix while the *S*-initiator induces a right-

handed *P*-helix. This can be concluded by the maxima or minima around 220 nm. A negative CD signal at 220 nm indicates a right-handed structure similar to a right-handed alpha helix while a positive maximum of the CD signal at this wavelength indicates a left-handed helical structure.

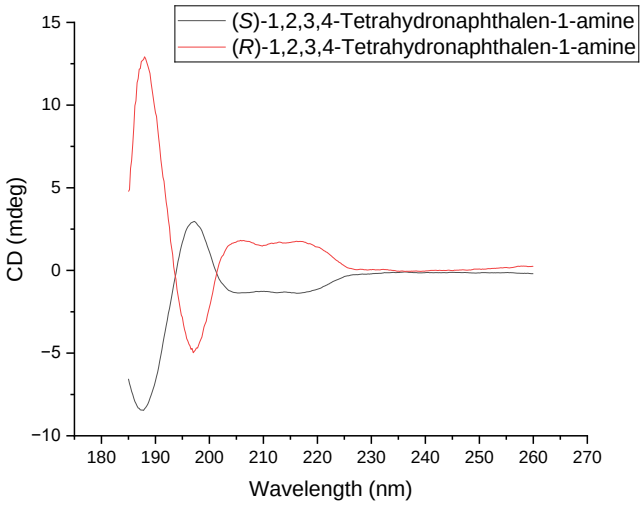

Figure SI 1: CD spectra of the initiators *R*- and *S*-1,2,3,4-tetrahydronaphthalen-1-amine used as initiators for the polymerization of Aib-NCA.

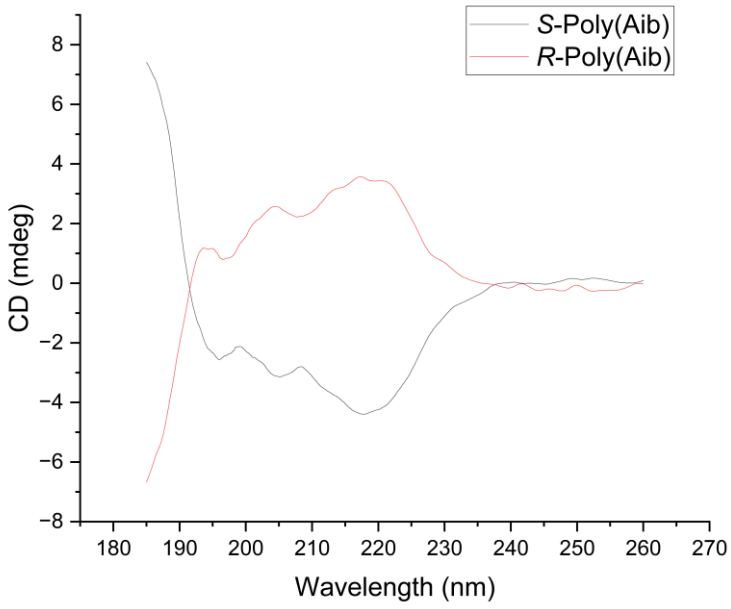

Figure SI 2: CD spectra of the *R*- and *S*-Poly(Aib) with the CD signals mirroring each other at the CD=0 line which proves a opposite handedness of these structures.

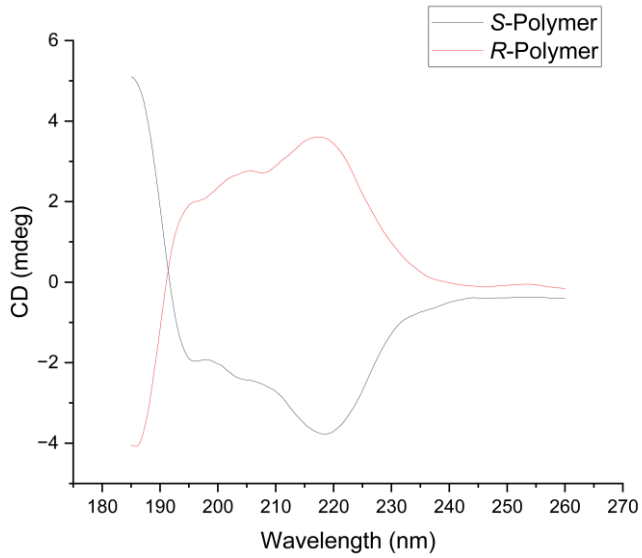

Figure SI 3: CD spectra of the *R*- and *S*-Polymer with the CD signals mirroring each other at the CD=0 line which proves a opposite handedness of these structures. The overall CD spectra is not significantly changed due to the post functionalization of the *R*- and *S*-Poly(Aib).

4.2. IR data

IR spectroscopy was measured before and after the post functionalization of the polymer. All spectra were recorded in the solid state and show strong signals around 1650 and 1540 cm^{-1} which indicate the formation of a helical structure in the solid state. Furthermore, the overall spectra are unchanged after post functionalization and does not differ between the *R*- and *S*-initiated polymer.

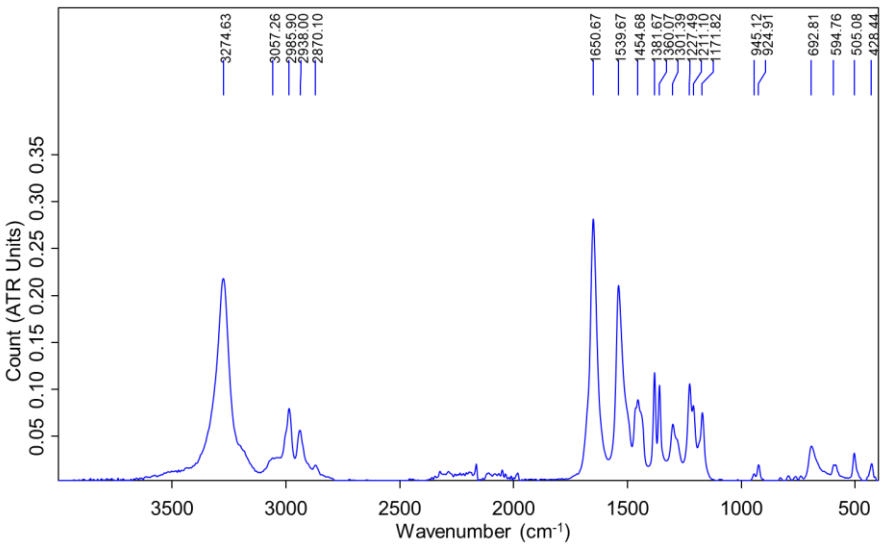

Figure SI 4: ATR-IR spectra of *R*-Poly(Aib) featuring IR signals at 1650 and 1539 cm^{-1} which are characteristic for a helical structure.

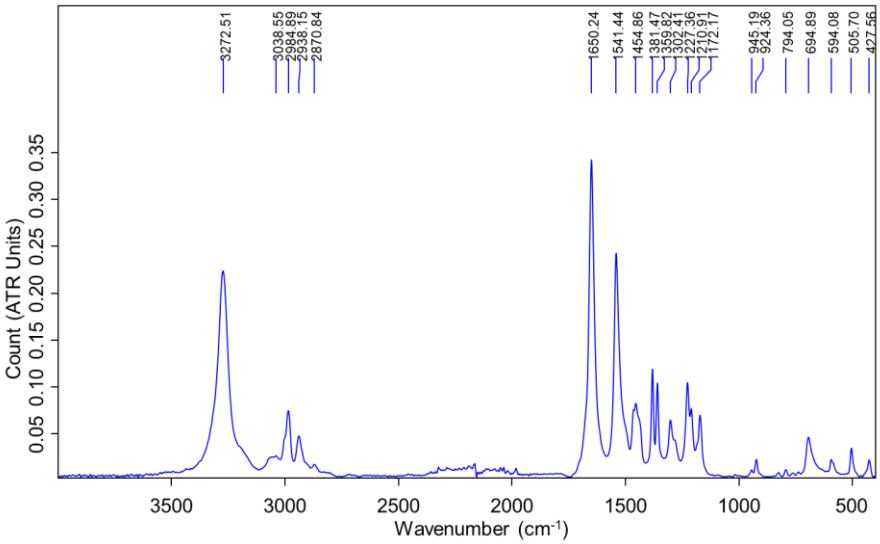

Figure SI 5: ATR-IR spectra of *S*-Poly(Aib) featuring IR signals at 1650 and 1541 cm^{-1} which are characteristic for a helical structure.

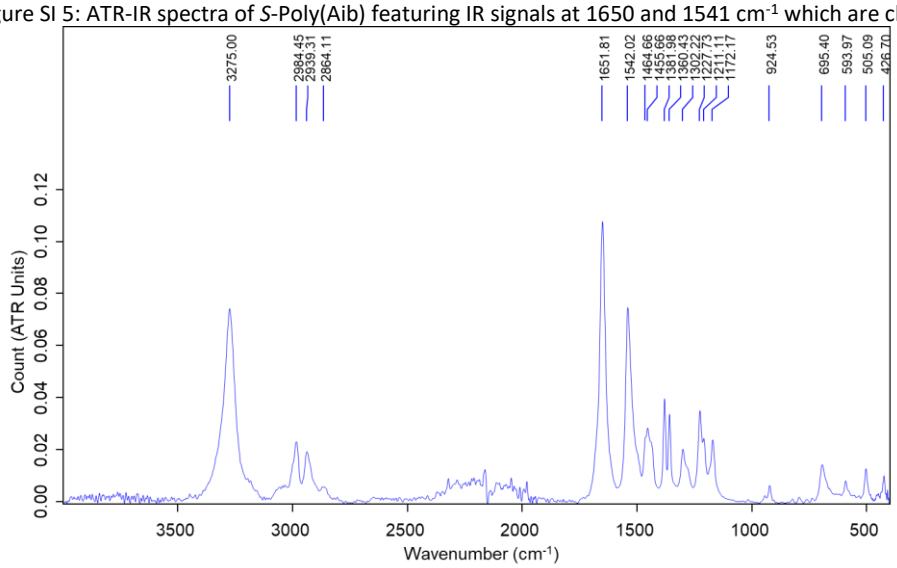

Figure SI 6: ATR-IR spectra of *R*-Polymer featuring IR signals at 1651 and 1542 cm^{-1} which are characteristic for a helical structure. The IR spectra is unchanged in comparison to the *R*-Poly(Aib) without isolipoic acid end group.

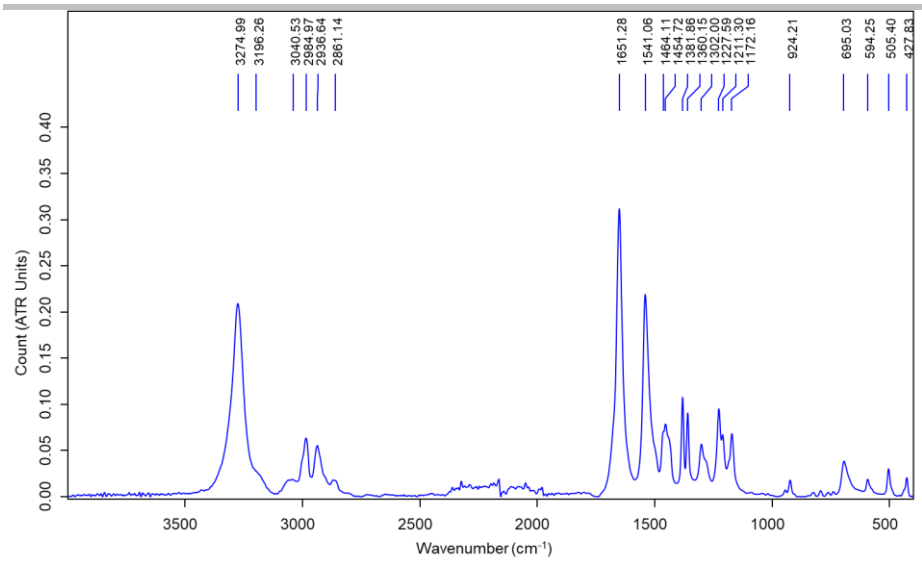

Figure SI 7: ATR-IR spectra of *S*-Polymer featuring IR signals at 1651 and 1542 cm^{-1} which are characteristic for a helical structure. The IR spectra is unchanged in comparison to the *S*-Poly(Aib) without isolipoic acid end group.

4.3. GPC data

The *R*-/*S*-Poly(Aib) and *R*-/*S*-Polymer were investigated with GPC to determine the average molecular weight and the polydispersity index (PDI). All polymers were dissolved in a HFIP and a PMMA calibration was used. The *R*-/*S*-Poly(Aib) have a slightly lower molecular weight in comparison to the post functionalized *R*-/*S*-Polymers while the PDI was changed only slightly. The overall shape for all samples show a peak around 11.2 ml retention volumes and a low intensity tail like shape in the lower retention volume (higher molecular weight) direction.

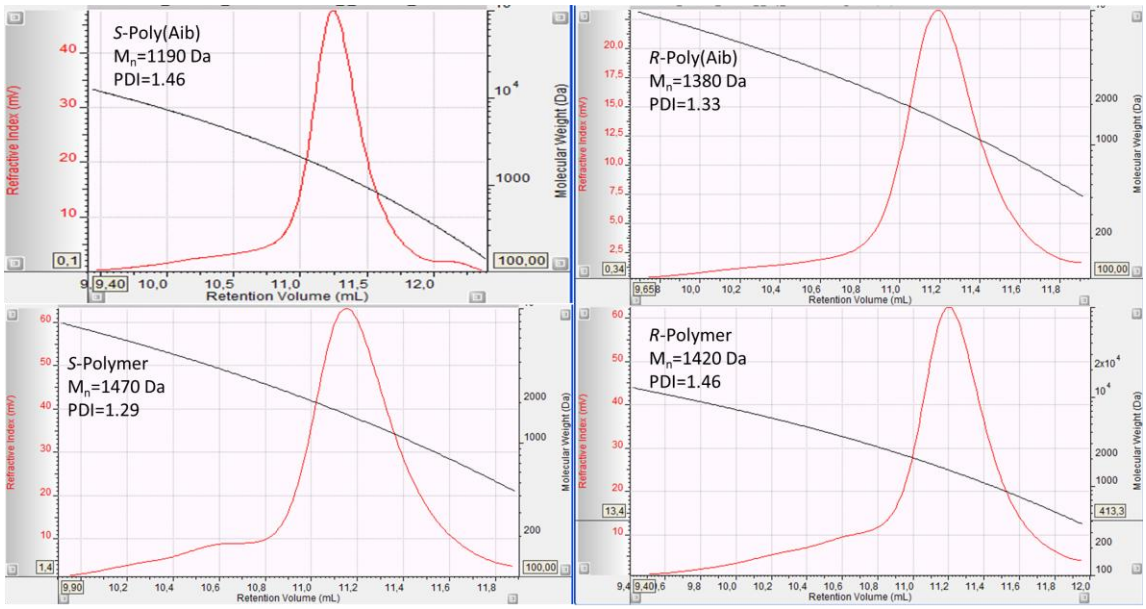

Figure SI 8: GPC measurements of *R*- and *S*-Poly(Aib) (upper row) and *R*- and *S*-Polymer (lower row) with the corresponding molecular weights and polydispersity index (PDI).

4.4. NMR data

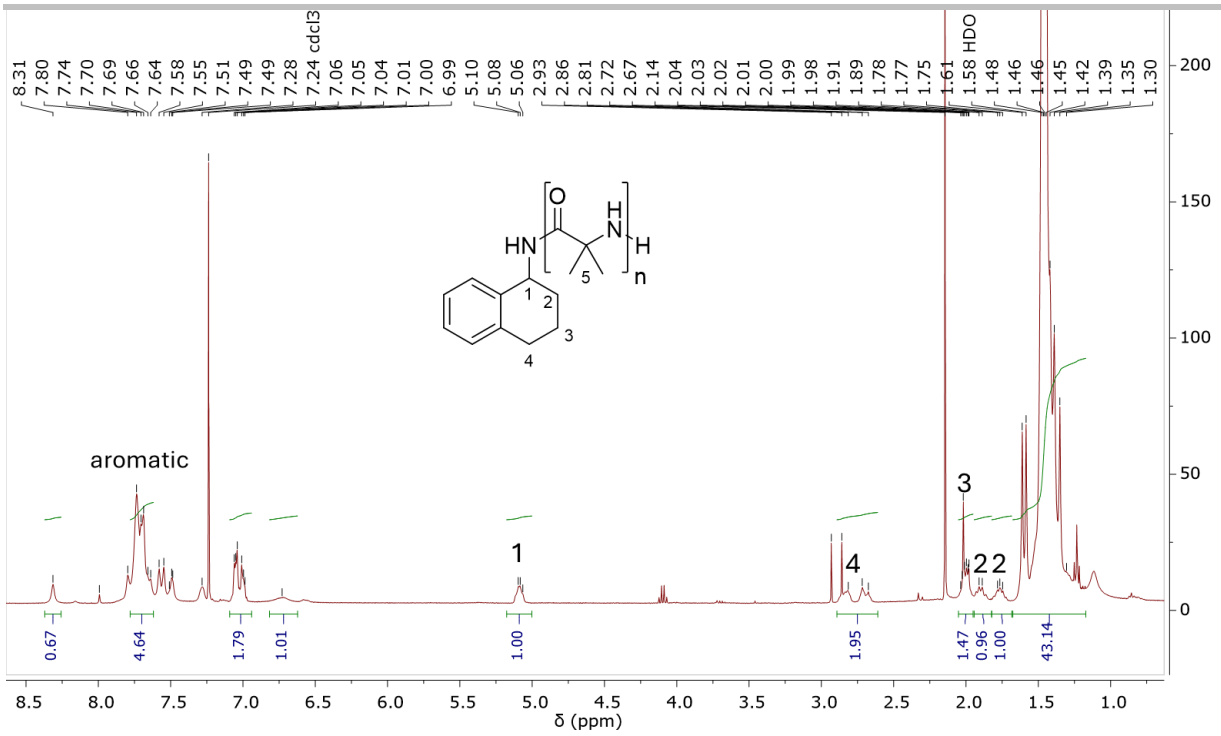

Figure SI 9: ^{1}H-NMR in $CDCl_3$ of Poly(Aib) with the peaks of the initiator visible and the isolated signal 1 used as a reference.

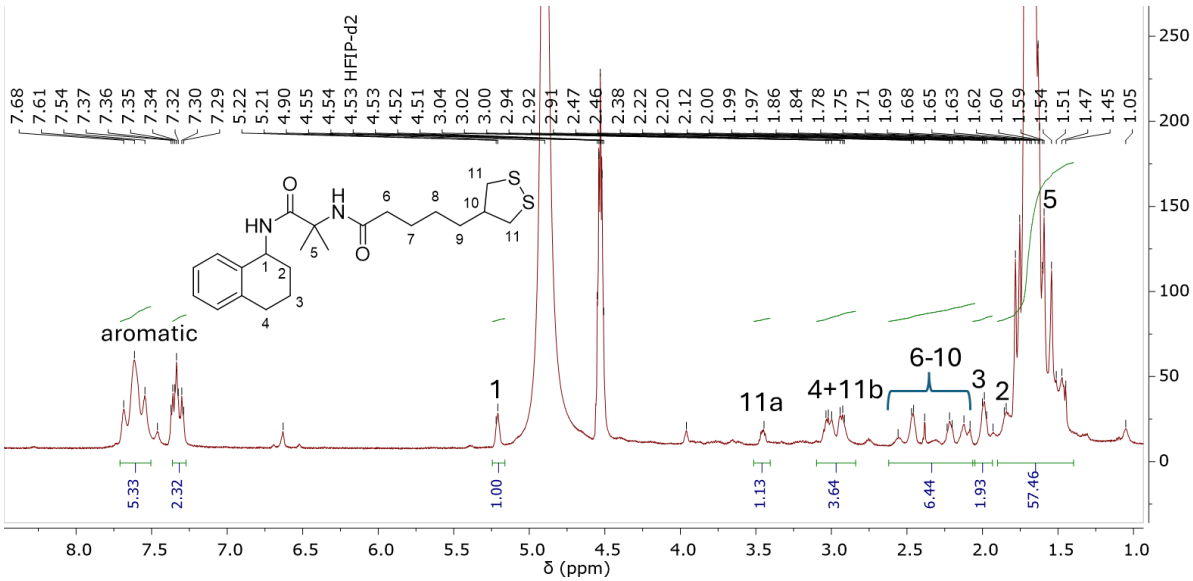

Figure SI 10: ^{1}H-NMR in deuterated HFIP of the Poly(Aib) with post functionalization with the peaks of the initiator visible as well as new signals which derive of the isolipoic acid end group and the isolated signal 1 used as a reference

4.5. MALDI-ToF MS data

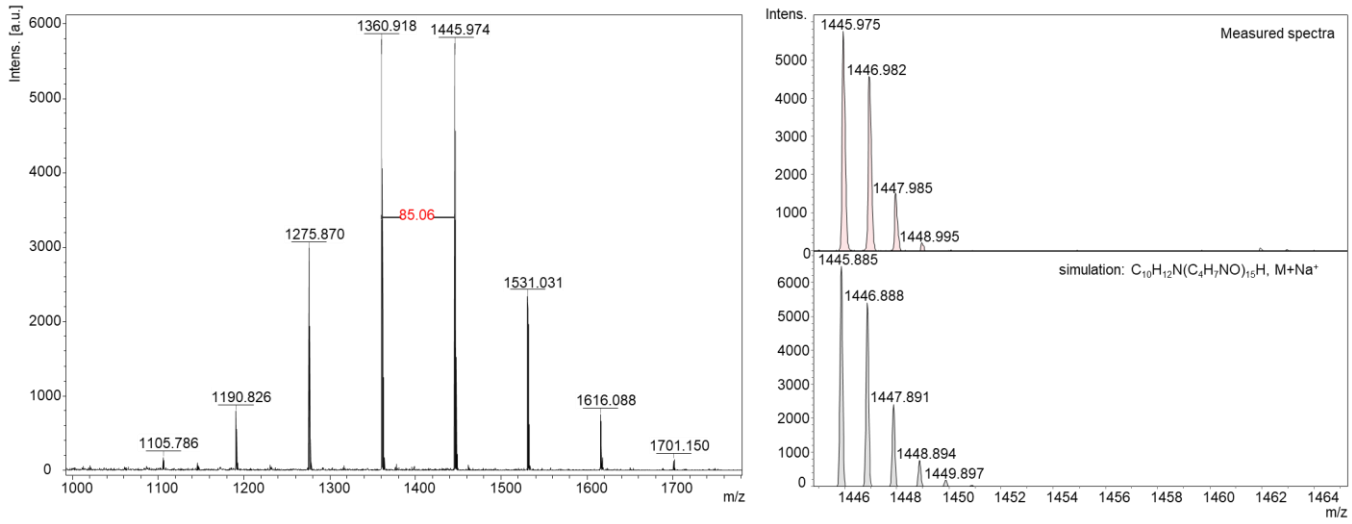

Figure SI 11: MALDI-ToF MS of *S*-Poly(Aib) with the simulation of the peak matching well to the desired product with a sodium ion.

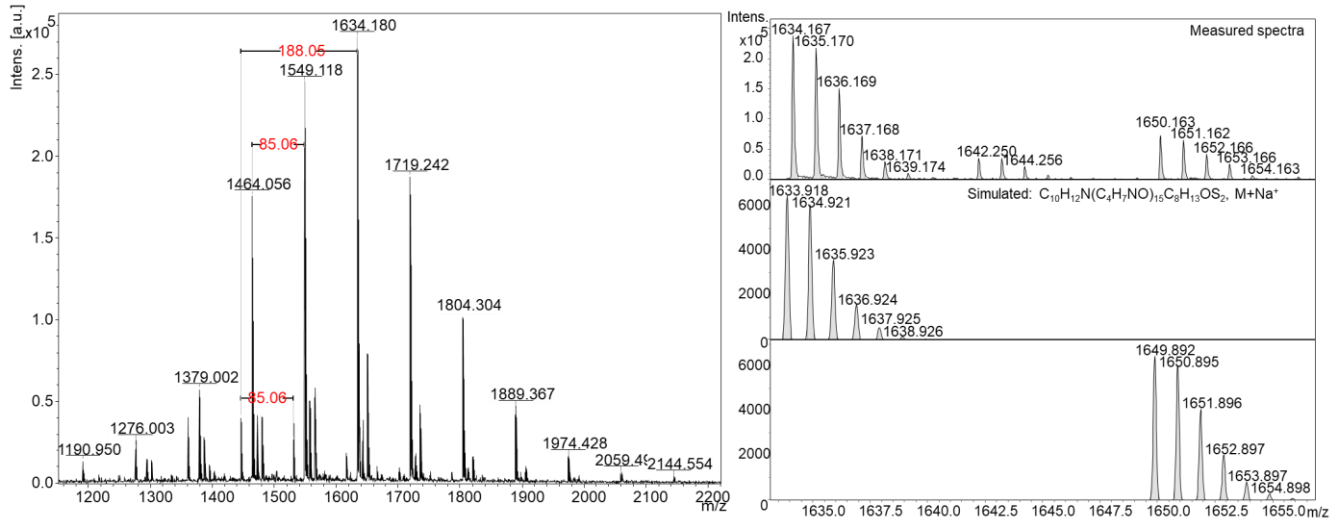

Figure SI 12: MALDI-ToF MS of *S*-Polymer with the simulation matching the measured peaks for the post functionalized Poly(Aib) with a sodium and potassium ion.

4.6. XPS data of the pure PMA substrate

The XPS measurement of the PMA substrate without polymer shows high intensity gold signals which was expected as this is the uppermost layer. Weak Cobalt and Nickel peaks can be observed as well proving the existence of the PMA layer in close proximity to the surface.

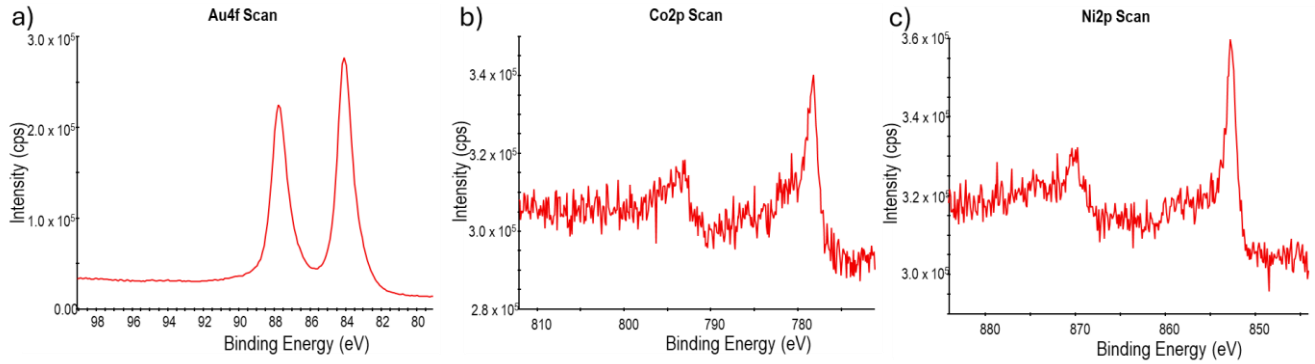

Figure SI 13: XPS measurements of the PMA substrate without polymer showing **a** strong gold peaks as well as **b** Cobalt and **c** Nickle peaks.

4.7. C-AFM of the pure PMA substrate

To ensure the quality of the c-AFM tip is similar before and after the c-AFM measurements of the polymer, c-AFM measurements of the pure gold surface of the PMA substrate without polymer were conducted before and after the polymer investigations. The results are shown in figure S13 with a maximum around 7000 nA at 0.2 V and a minimum of around -7500 nA at -0.2 V. The conductivity is not significantly reduced after the polymer investigations and displayed together with the measurements before. The pure gold surface of the PMA substrate has a conductivity of at least 10 times the polymer coated substrate.

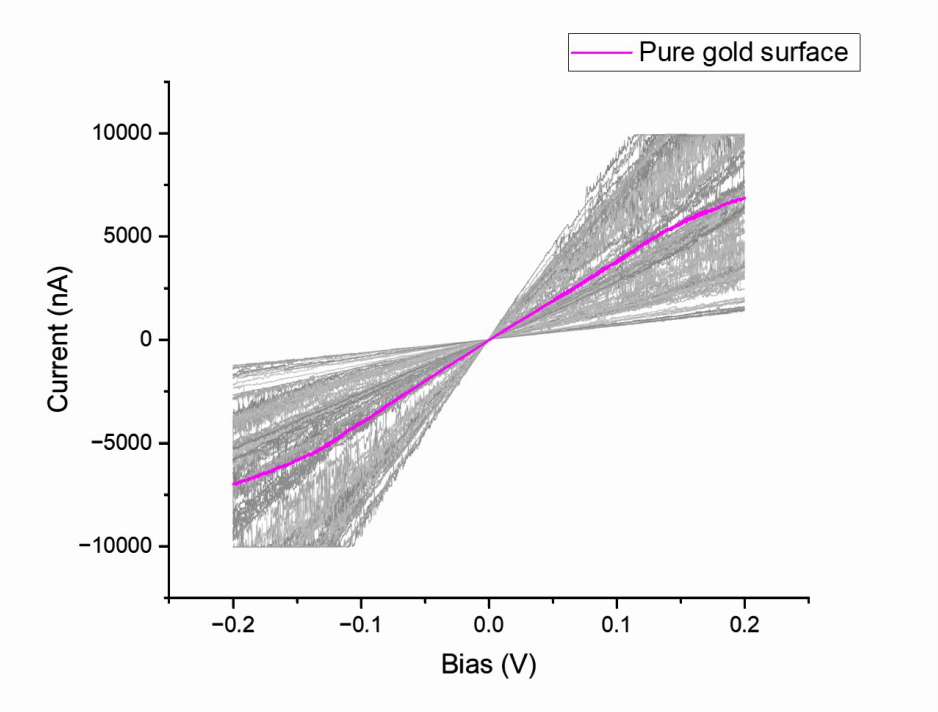

Figure SI 14: c-AFM measurements for the pure gold surface without polymer conducted before and after the c-AFM measurements of polymers. The variation of the individual measurements is quite big and displayed as a grey area behind the average displayed in purple.

4.8. Polymer layer thickness determination via AFM

To determine the exact thickness of the polymer layer two different approaches were probed (see figure SI 14), either using a reference structure composed of MgO displaying a height of around 6 nm and edges of roughly 14 nm in height. After self-assembly of the polymer monolayer on the PMA substrate gold surface AFM showed a rough area around the unchanged MgO spots. The middle of the MgO spots was roughly the same height as the polymer monolayer around it which is around 6 to 8 nm. A second, more direct approach was probed by first growing the self-assembled polymer monolayer on the surface and afterwards removing part of the polymer layer with concentrated hydrochloric acid, then exposing half of the substrate in the acid solution for 1 min followed by carefully rinsing the surface with water. The artificial edge created by this procedure revealed a height of the monolayer of 6 nm, which is in good agreement to the results of the previous method and inline with the expected dimensions of the helical polymer.

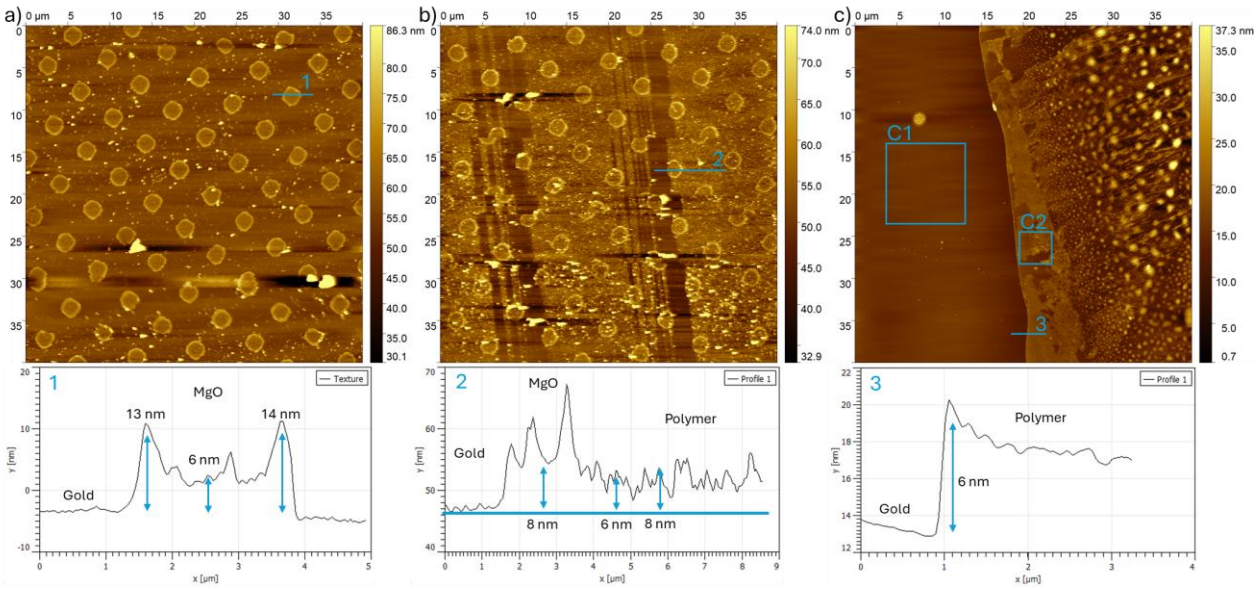

Figure SI 15: Determination of the thickness of the polymer layer **a** MgO spots were placed on the surface of the PMA substrate and the height profile is given. It can be seen that the edges of the spot are elevated compared to the middle part. **b** After polymer deposition a new area with a with different roughness was observed. Conveniently there was also a small stripe without any polymer so a height profile over the native gold surface, the MgO spot and the newly formed polymer film could be given. The monolayer height was determined to be between 6 to 8 nm. **c** PMA substrate with polymer film after dipping in concentrated HCl solution. On the left side (C1) the unmodified gold surface can be seen with an average roughness of 330 pm while the highlighted area on the right (C2) gives an average roughness of 1.23 nm. The height profile over this artificial edge shows a monolayer height of around 6 nm.

5. Supplementary References

[1] aM. Rohmer, Ö. Ucak, R. Fredrick, W. H. Binder, *Polymer Chemistry* **2021**, *12*, 6252-6262; bM. Rohmer, S. G. Ebbinghaus, K. Busse, J. Radicke, J. Kressler, W. H. Binder, *Chemistry – A European Journal* **2023**, *n/a*, e202302585; cJ. Freudenberg, W. H. Binder, *Acs Macro Lett* **2020**, *9*, 686-692.